Development of Lattice-Based Panels via Direct Metal Laser Sintering (DMLS) for Satellite Applications

Emmanuel Arriola *, Jozal Carrido, Mark Francis Sedano, Ulysses Ante, Prince William Lim, Arvin Oliver Ng, Renzo Wee, Roider Pugal, Toni Beth Lopez

Posted Date: 28 April 2026

doi: 10.20944/preprints202604.1882.v1

Keywords: Direct Metal Laser Sintering; lattice structures; topology optimization; AlSi10Mg

 doi:10.20944/preprints202604.1882.v1

Article

Development of Lattice-Based Panels via Direct Metal Laser Sintering (DMLS) for Satellite Applications

Emmanuel Arriola [1,*], Jozal Carrido [1], Mark Francis Sedano [1], Ulysses Ante [1], Prince William Lim [2], Arvin Oliver Ng [2], Renzo Wee [2], Roider Pugal [2] and Toni Beth Lopez [1]

[1] Department of Science and Technology - Metals Industry Research and Development Center, Taguig City, 1631, Philippines

[2] Spacecraft Mechanical and Autonomous Development Division, Philippines Space agency, Quezon City, Philippines

* Correspondence: erarriola@outlook.com

Featured Application

This research applies Direct Metal Laser Sintering (DMLS) to produce lightweight, lattice-based mounting panels for the PHL-50 Bus microsatellite. By replacing traditional rib-type boards with an optimized Body-Centered Cubic (BCC) architecture, this approach creates an integrated, adhesive-free component. Ultimately, it offers a customizable, mass-optimized solution for securing payloads that meets strict aerospace structural standards.

Abstract

This study explores the development of lattice-based panels for satellite applications using Direct Metal Laser Sintering and aimed to optimize lightweight, high-strength structures suitable for CubeSat deployment. Three lattice configurations namely Body-Centered Cubic, Octet, and Gyroid were evaluated. While Gyroid lattices exhibited the highest compressive strength at 13,825.8 N, the BCC lattice was selected for the final design due to superior manufacturability and weight reduction potential. The final optimized panel weighed 185.7 g, achieving an 11.4% reduction from the initial rib-type design and a 65.2% reduction from a solid panel. Finite Element Analysis and mechanical testing confirmed that the fabricated structures met the necessary mechanical requirements for aerospace launch conditions.

Keywords: Direct Metal Laser Sintering; lattice structures; topology optimization; AlSi10Mg

1. Introduction

The design and fabrication of structural components for satellite applications are driven primarily by the strict mass limitations imposed by launch providers. Lightweighting is a critical consideration, as reducing the structural mass of spacecraft components allows for budget reallocation toward high-value avionics and payloads, ultimately enhancing mission capabilities [1]. Consequently, the aerospace industry continually seeks mass-optimization strategies that do not compromise structural integrity [2].

Lattice-based panels present a viable solution for this mass optimization [3]. These structures typically employ a sandwich-type assembly consisting of two face sheets separated by a lightweight core material, offering high stiffness-to-weight ratios [4]. However, conventional sandwich panels, such as those with aluminum honeycomb cores, present significant manufacturing challenges (Figure 1). They are often expensive to produce and difficult to manufacture locally, creating reliance on complex supply chains. Furthermore, traditional assembly requires adhesives to bond external sheets to the core, which adds processing steps and potential failure points [5].

 doi:10.20944/preprints202604.1882.v1

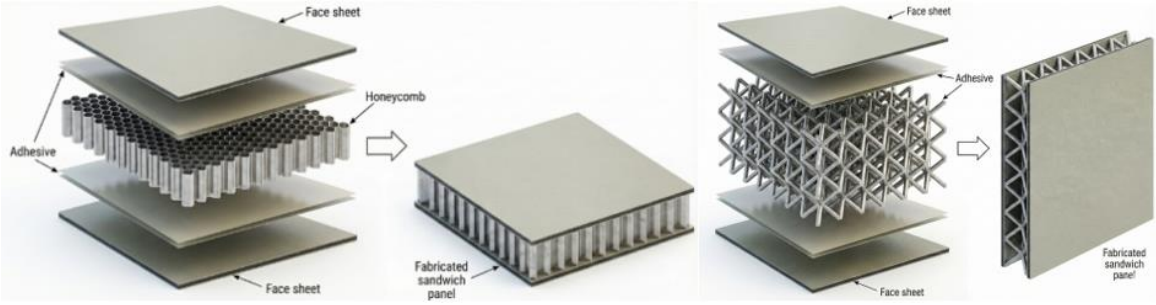

Figure 1. Comparison of honeycomb panel and lattice-based panel.

Additive Manufacturing (AM), specifically Direct Metal Laser Sintering (DMLS), offers a transformative approach to overcoming these limitations [6]. By leveraging AM, it is possible to fabricate panels with an integrated lattice core and thin external sheets in a single production run, eliminating the need for adhesives and simplifying the manufacturing process [7]. This study aims to develop lightweight, structurally sound panels by harnessing local expertise in AM and structural design. This seeks to demonstrate the feasibility of locally developed, 3D-printed lattice-based panels for satellite deployment.

This research explores specific lattice architectures belonging to the family of cellular solids, categorized into strut-based lattices and triply periodic minimal surface (TPMS) structures. Strut-based lattices, specifically Body-Centered Cubic (BCC) and Octet configurations, were investigated for their mechanical stability. Additionally, the Gyroid lattice, a TPMS structure, was evaluated due to its unique porous geometry with zero mean curvature. While Gyroid lattices are characterized by smooth struts and spherical cores that are often self-supporting which are for enhancing their printability, they present challenges regarding unit cell size and the necessity for exit pathways to remove trapped powder post-printing [8].

The fabrication of these complex geometries was conducted using the EOS M290 DMLS 3D printer. Various printing parameters were examined to determine the optimal settings for balancing mechanical performance with manufacturability.

The design and optimization efforts in this study focused on a mounting panel intended for the PHL-50 Bus. The panel serves a critical dual purpose that must provide the necessary structural rigidity to securely mount electronic component assemblies while adhering to strict weight constraints. In its initial configuration, the component utilized a rib-type design to achieve structural stiffness, weighing 209.6 g when modeled with AlSi10Mg. The optimization of this component is vital, as it must withstand specific loading conditions and environmental factors inherent to space launch and operation.

To achieve the necessary weight reduction without compromising structural integrity, this study explores the use of lattice structures. Lattice structures are defined as interconnected unit cells arranged spatially within a volume and belong to the broader family of cellular solids [9]. These structures are categorized by various configurations, including 2-dimensional versus 3-dimensional, open-cell versus closed-cell, and homogeneous versus heterogeneous arrangements. The classification focuses on two primary architecture categories: strut-based lattices and TPMS as listed in Table 1.

Table 1. Three lattice structure evaluated with its features.

Name	Lattice Structure	Feature

 doi:10.20944/preprints202604.1882.v1

Body-Centered Cubic (BCC)	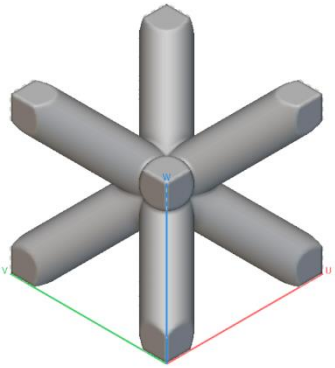	A strut-based lattice known for mechanical stability.
Gyroid	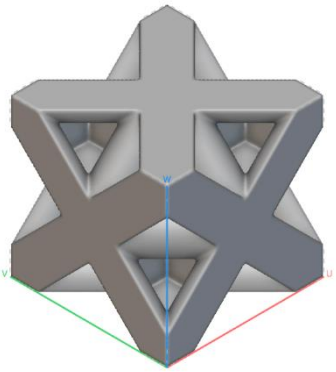	A Triply Periodic Minimal Surface (TPMS) structure valued for its self-supporting geometry and zero mean curvature.
Octet	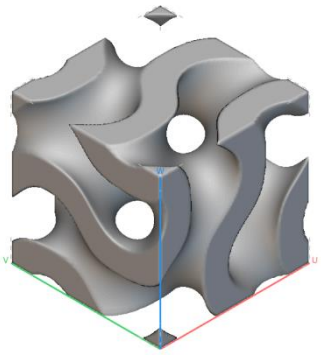	A strut-based lattice providing high stiffness.

1.1. Strut-Based Lattices

These architectures are characterized by their mechanical stability and truss-like connections. Common examples include the Body-Centered Cubic (BCC), Face-Centered Cubic (FCC), Diamond, and Octet lattices. This study specifically investigated BCC and Octet lattices for their suitability in replacing the solid volume of the satellite panel.

1.2. TPMS Lattices

Unlike strut-based designs, TPMS structures such as the Gyroid and Diamond are porous geometric arrangements defined by zero mean curvature [8]. The Gyroid lattice, for instance, is mathematically defined by the equation:

$$\boldsymbol{F(x,y,z) = cos(x)sin(y) + cos(y)sin(z) + cos(z)sin(x) + a} \quad (1)$$

TPMS structures are often preferred in additive manufacturing because they are self-supporting, characterized by smooth struts and spherical cores. However, they present unique manufacturing challenges, specifically regarding unit cell size limitations and the requirement for exit pathways to remove trapped material from the pores post-printing.

1.3. Potential of 3D-Printed Satellite Structures

 doi:10.20944/preprints202604.1882.v1

The utilization of AM to produce these lattice-based satellite structures offers distinct advantages over traditional manufacturing. Research indicates that AM lattice panels can withstand real launch conditions comparable to traditional aluminum honeycomb panels [10–12]. Key desirable properties realized through this approach include an excellent stiffness-to-weight ratio, high strength at joints, and a reduced number of structural connections, all achieved within a shorter fabrication cycle. By integrating the lattice core and face sheets into a single printed part, the need for adhesives is eliminated, simplifying production and mitigating potential points of failure.

2. Methodology

The methodology followed a systematic workflow designed to transition from conceptualization to a fully verified prototype.

As defined in Figure 2, the process began with requirements definition and material selection, followed by an iterative design phase involving topology optimization and lattice generation. Designs were validated through Finite Element Analysis (FEA) before proceeding to prototyping via Direct Metal Laser Sintering (DMLS). The final phase involved post-processing and rigorous mechanical testing to characterize the lattice performance and ensure compliance with launch standards.

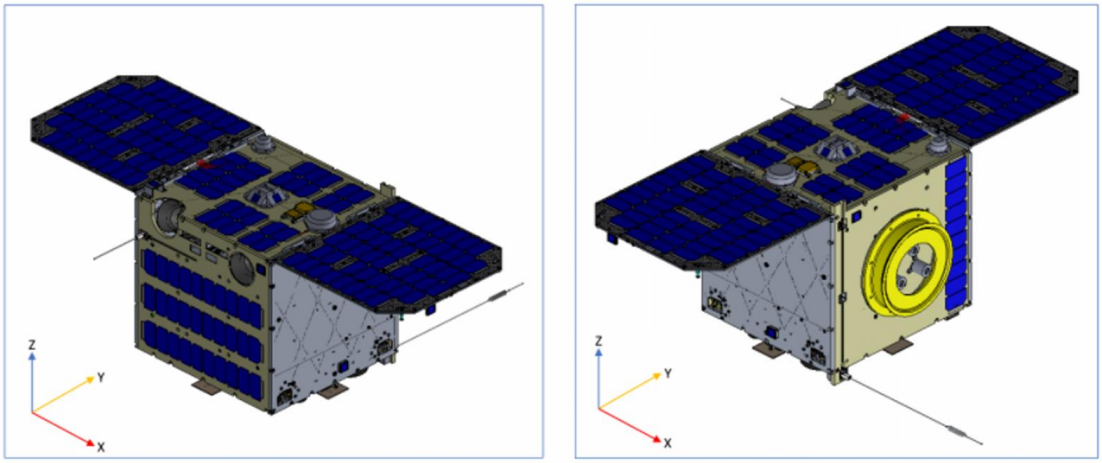

Figure 2. PHL-50 Microsatellite.

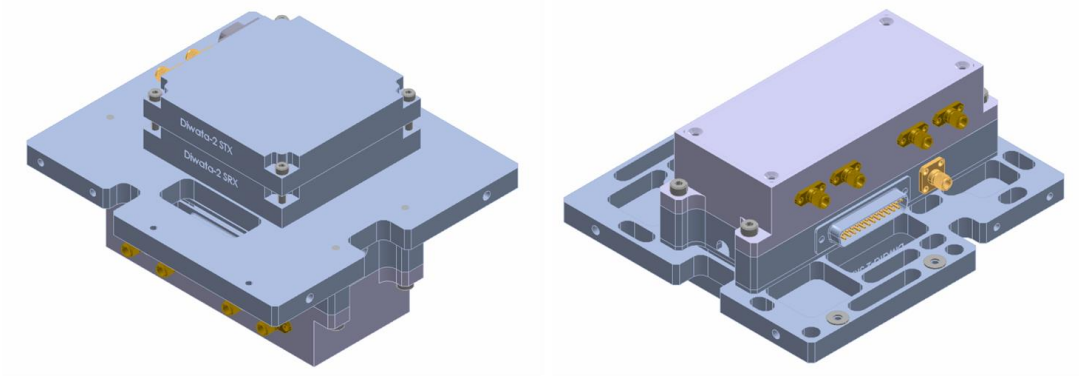

Figure 3. Mounting panel with electronic component assembly: top (left) and bottom (right) view.

 doi:10.20944/preprints202604.1882.v1

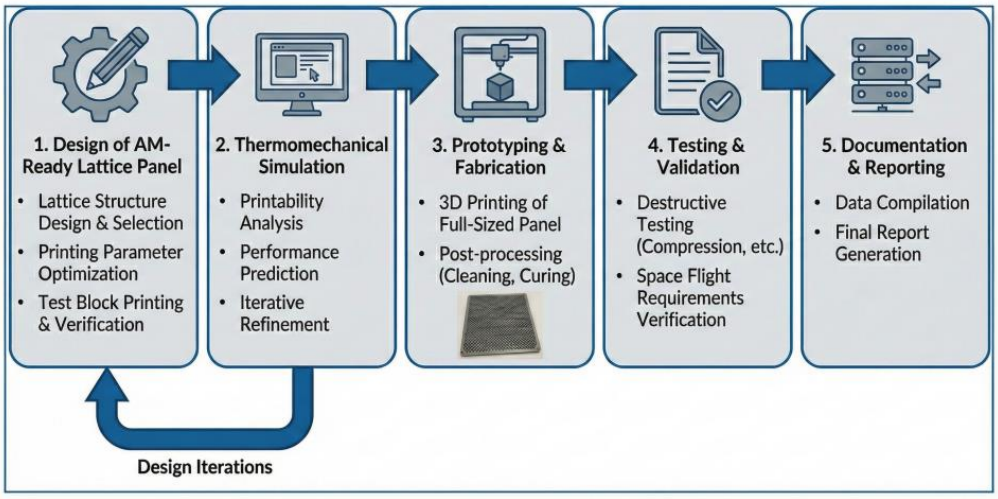

Figure 4. Methodology.

2.1. Requirements Definition and Material Selection

The primary objective was to develop an additive manufacturing-ready panel suitable for satellite applications, specifically designed to mount electronic components for the microsatellite. The design requirements were governed by strict mass limitations and structural integrity standards mandated for space launch. Compliance with Japan Aerospace Exploration Agency (JAXA) guidelines was central to the design process, dictating load conditions, dimensions, and tolerances to ensure compatibility with the JEM Payload Accommodation Handbook [13].

Initially, the material selected for the study was AlSi10Mg (Aluminum-Silicon-Magnesium alloy). This material was chosen due to its well-documented suitability for DMLS processes, favorable strength-to-weight ratio, and established use in aerospace applications [14,15].

2.2. Panel Design and Lattice Selection

The design process commenced with an initial rib-feature panel provided by the Philippine Space Agency (PhilSA), which weighed 209.6 g and relied on traditional ribbing for structural rigidity. To achieve significant weight reduction, the researchers transitioned from this solid-rib design to a lattice-based architecture.

Three specific lattice structures (Table 1) were selected for evaluation based on their mechanical properties and suitability for DMLS fabrication, Body-Centered Cubic (BCC), Octet, and Gyroid.

As for the design of the test specimens for the compressive tests, the researchers opted to use a 13 mm x 13 mm x 10 mm which includes 1 mm thickness of solid top and bottom faces while the middle section of the specimen is converted into a single layered cell or a three (3) layered cell of the selected lattice design. The parameters used for the lattice generation are listed in Table 2.

Table 2. Lattice generation parameters.

Parameters	BCC	Octet	Gyroid
Unit Cell	Body Centered Cubic	Octet	Gyroid
Orientation	UVW	UVW	UVW
Unit Cell Size	4 mm x 4 mm x 4 mm	4 mm x 4 mm x 4 mm	4 mm x 4 mm x 4 mm
Trim	Yes	Yes	Yes
Thickness	1 mm	1 mm	1 mm

2.3. Computational Design and Topology Optimization

CAD modeling and advanced lattice generation were performed using nTopology software, ensuring all designs met JAXA standards. The weight reduction strategy employed a two-stage

 doi:10.20944/preprints202604.1882.v1

topology optimization approach. First, a 2D model of the panel's middle section was optimized to identify critical load-bearing paths and reduce computing time. The optimization targeted a 50% mass reduction while maintaining "Exclusion Regions" for bolt holes and edges required for fastening to the satellite frame. Following the 2D analysis, the process advanced to a full 3D solid model. The optimization was driven by Structural Compliance to prioritize integrity.

The topology optimization was governed by JAXA standards, utilizing a 9G load condition for the initial optimization of the panel. This value was applied to simulate the forces the panel would endure during launch. The optimization considered various combinations of force component directions (±5Gx, ±6Gy, and ±5Gz) to account for the unpredictable tumbling of the satellite in space, resulting in multiple design iterations that were consolidated to form the final profile.

2.4. Simulation and Validation

Finite Element Analysis (FEA) was conducted within nTopology to simulate the structural behavior of the lattice panels under operational stress. While the initial optimization used 9G loads, verification simulations utilized revised load conditions provided by PhilSA (±5Gx, ±6Gy, and ±5Gz) to validate printability and performance under specific force magnitudes. Static analysis was performed to identify high-stress areas, particularly around bolt holes, ensuring the maximum Von Mises stress did not exceed the yield strength of the AlSi10Mg material.

2.5. Prototyping via Direct Metal Laser Sintering (DMLS)

Fabrication was executed using an EOS M290 DMLS 3D printer. STL files were prepared using Materialise Magics, where support structures were generated and print orientation was optimized to minimize support volume.

A layer height of 30 microns was selected for the lattice components to ensure fine detail and smoother surface finish, compared to an initial trial at 40 microns. A soft recoater blade was utilized specifically to prevent damage to the delicate lattice struts during powder spreading. The printing environment was continuously monitored, maintaining an argon atmosphere to prevent oxidation and strictly controlling chamber pressure and temperature.

2.6. Post-Processing

Upon completion of the print cycle, excess powder was removed using a wet separator while the parts remained attached to the build plate and to eliminate residual stresses from the thermal cycles of printing, the parts were heat-treated in a furnace at 300°C for 2 hours after that parts were separated from the build plate using a wire cutting machine.

2.7. Testing and Characterization

The study employed comprehensive testing to verify both mechanical properties and dimensional accuracy. A Universal Testing Machine (UTM) was used to conduct compressive and tensile tests on designated test coupons (Figure 5). This characterized the maximum load-bearing capacity of the different lattice types.

 doi:10.20944/preprints202604.1882.v1

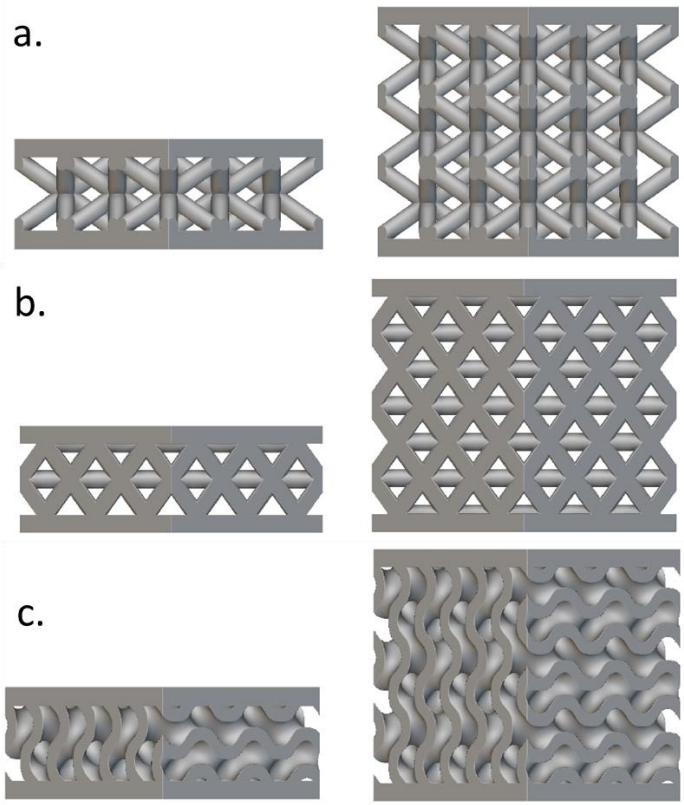

Figure 5. (a) BCC Compressive Specimen Design: Single Cell Layer (left) and Three-Layered Cell (right), (b) Octet Compressive Specimen Design: Single Cell Layer (left) and Three-Layered Cell (right), (c) Gyroid Compressive Specimen Design: Single Cell Layer (left) and Three-Layered Cell (right).

Dimensional accuracy was verified using a vernier caliper to compare the printed dimensions against the original CAD model. Additionally, a "fit check" was performed by assembling the printed panel with the actual PHL-50 bus microsatellite frame and components to confirm interface tolerance and alignment. To inspect the quality of the fine lattice features, optical equipment was used to observe individual struts. This inspection revealed residual AlSi10Mg powder adhering to the lattice members, highlighting areas for potential cleaning process improvements.

3. Results and Discussion

3.1. Topology Optimization and Design Evolution

The weight reduction of the panel involves topology optimization to determine which sections of the panel are only needed based on the loading constraints. To achieve this, PhilSA used a 2D model of the middle section of the panel to determine the necessary sections and to reduce computing time necessary for the simulation. Table 3 shows the initial loading constraints provided by PhilSA in consideration of the center of gravity of the electronic components mounted on the panel.

 doi:10.20944/preprints202604.1882.v1

Table 3. Loading constraints in consideration of the center of gravity of the electronic components mounted on the panel.

Designation	Force Location			Force Component Magnitude		
	X	Y	Z	X	Y	Z
Remote Force 1	9.24 mm	- 6.39 mm	- 15.25mm	± 20.54 N	± 20.54 N	± 20.54 N
Remote Force 2	- 5.08 mm	- 4.41 mm	32.2 mm	± 36.67 N	± 36.67 N	± 36.67 N

As for the constraints shown in Figure 6, "Displacement Components" was identified which in actuality will be secured with fasteners into the frame of the PHL-50. In addition, these edges were also identified as "Exclusion Regions" for the topology optimization process. Lastly, a 50% Mass Reduction was selected for the topology optimization process.

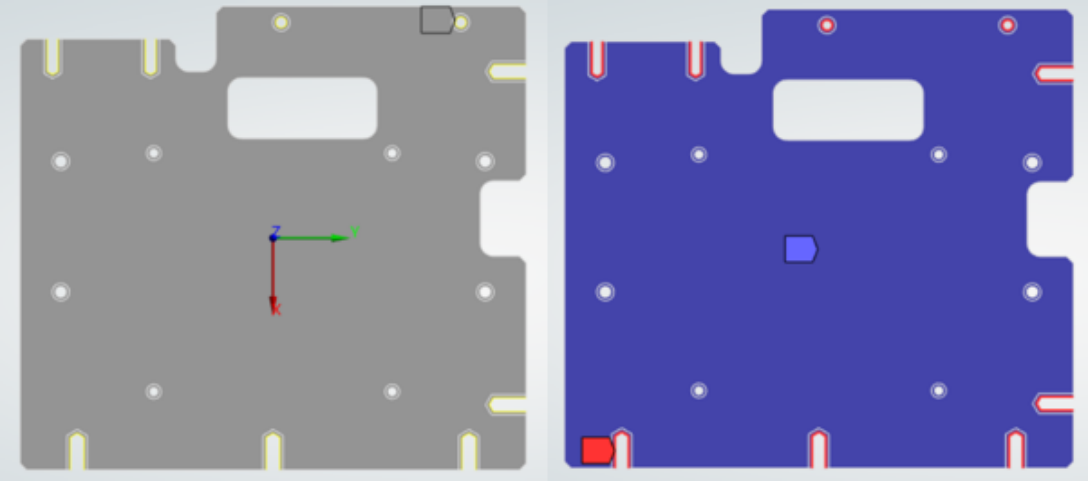

Figure 6. Displacement Constraints (left) and Exclusion Regions (right) for 2D Simulation.

It is important to consider all possible combinations of signs of the force component magnitudes since the panel will be subjected to forces in different directions during tumbling in space.

Once all designs were generated, the researchers overlapped the designs together (Figure 7) to obtain the necessary profile that can withstand all directions of the force components. It was then extruded to 10 mm to meet the panel's thickness requirement. The result was a part weighing 440.6 g with a 17.38% weight reduction from the solid converted part weighing 533.3 g using AlSi10Mg material.

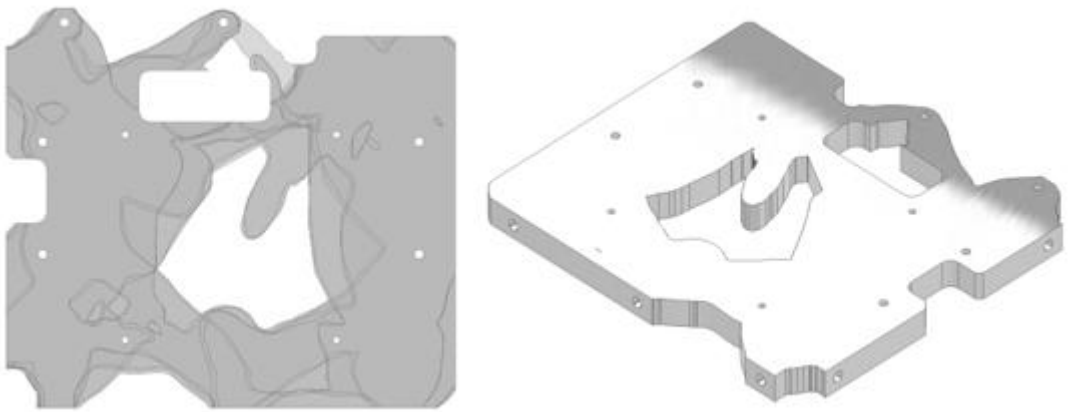

Figure 7. Consolidated Topology Optimized Panel Design.

 doi:10.20944/preprints202604.1882.v1

However, this design is still heavier than the original rib type design by 52.43%. To address this, the researchers opted to convert the design into lattice-based through nTopology software. The selected lattice designs for minimal weight are BCC and Octet. The profile generated from the topology optimization designs which are load bearing regions are to be converted to high-density lattice while the reduced regions of the panel are to be converted to low-density lattice. In addition, the design will keep the design features of the identified in Figure 8 "Exclusion Regions", bolt holes and top face with 2 mm offset. Table 4 shows the parameters for the lattice density generation.

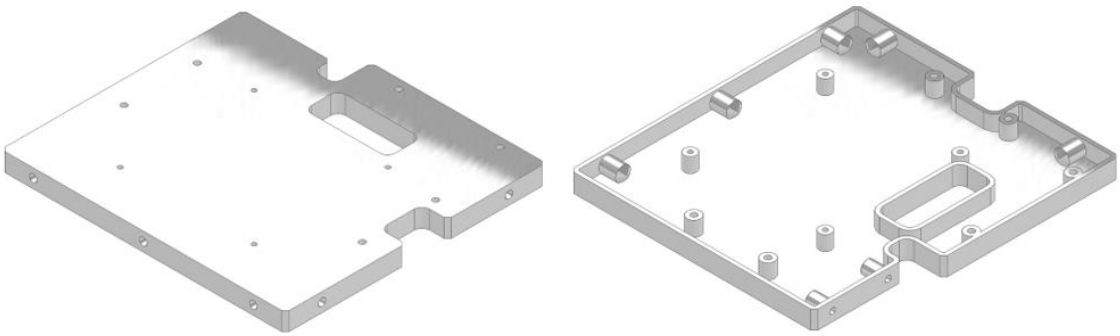

Figure 8. Lattice Exclusion Regions of the panel: top (left) and bottom (right).

Table 4. Parameters for Lattice Panel Density Generation.

Parameters	High-density Lattice	Low-density Lattice
Orientation	UVW	UVW
Unit Cell Size	5 mm x 5 mm x 5 mm	10 mm x 10 mm x 5 mm
Thickness	1 mm	1 mm

The result of the conversion (illustrated in Figure 9) was a panel design weighing 161 g for BCC lattice and 242.3 g for Octet lattice using AlSi10Mg material in the nTopology software. The BCC design is lighter than the original rib type by 23.19%, however the Octet design weighs 13.5% more than the original rib type.

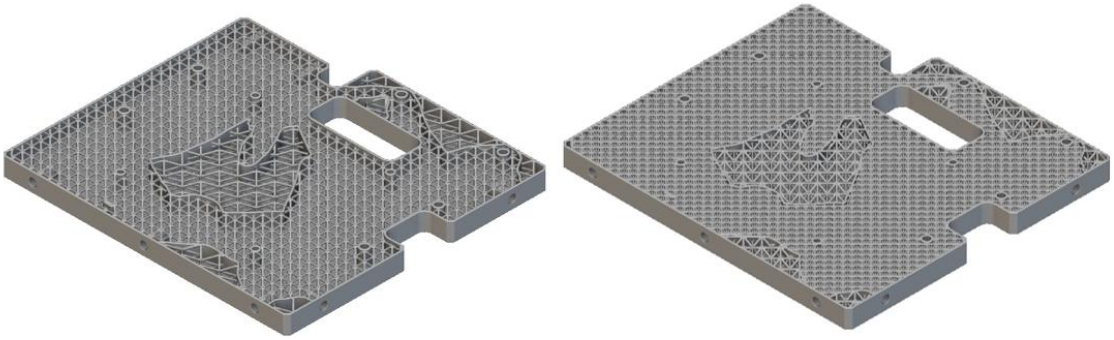

Figure 9. BCC Lattice Design 1 (left) and Octet Lattice Design 1 (right).

3.2. Lattice Conversion and Final Design Selection

To surpass the weight efficiency of the original rib-type design, the optimized solid geometry was converted into lattice structures. The study focused on Body-Centered Cubic (BCC) and Octet lattices due to their potential for minimal weight. The design strategy utilized a variable density approach: load-bearing regions identified during topology optimization were assigned high-density lattices (5×5×5 mm unit cells), while non-critical regions received low-density lattices (10×10×5 mm unit cells).

 doi:10.20944/preprints202604.1882.v1

The initial conversion yielded a BCC panel weighing 161 g and an Octet panel weighing 242.3 g. While the BCC design achieved a 23.19% weight reduction compared to the original 209.6 g rib-type design, the Octet design proved 13.5% heavier.

The optimized designs in Figure 10 are then merged into one part through a CAD Modeling Software. In addition, the shell perimeter of the panel along with the bolt holes necessary for the mounting of the components were merged with the optimized design to provide the panel with the proper fitting in the PHL-50 frame.

Figure 10. BCC Lattice Design 1 (left) and Octet Lattice Design 1 (right).

To verify the design, the researchers subjected the merged optimized design to the revised loading conditions provided by PhilSA through Finite Element Analysis in nTopology. The result of the static analysis has shown that the areas that have the highest loads are along the bolt holes of the panel. However, the maximum stress generated by the loading conditions is 6.35 Pa ask shown in Figure 11 which is safe against the material's tensile and yield strength using EOS' AlSi10Mg. This result shows that the panel needs to be reinforced in the bolt hole areas.

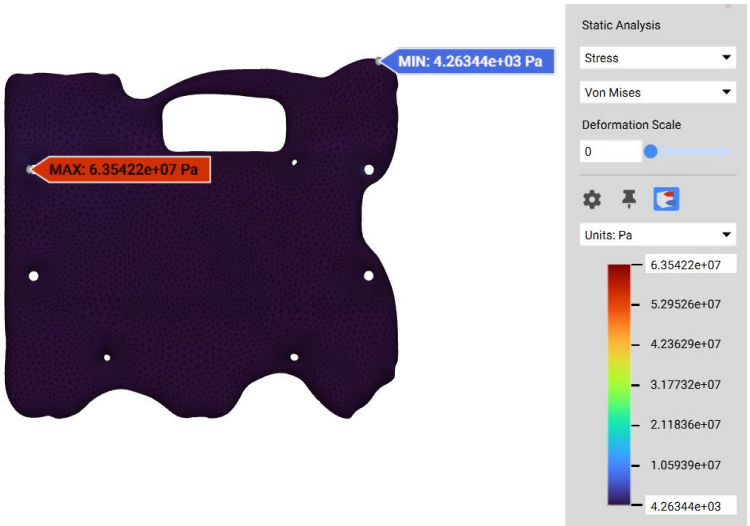

Figure 11. Finite Element Analysis verification of topology optimized panel.

Upon completion and verification, the design was exported as a STEP file. The researchers added this feature shown in Figure 12 to the panel design through a CAD Modeling software.

 doi:10.20944/preprints202604.1882.v1

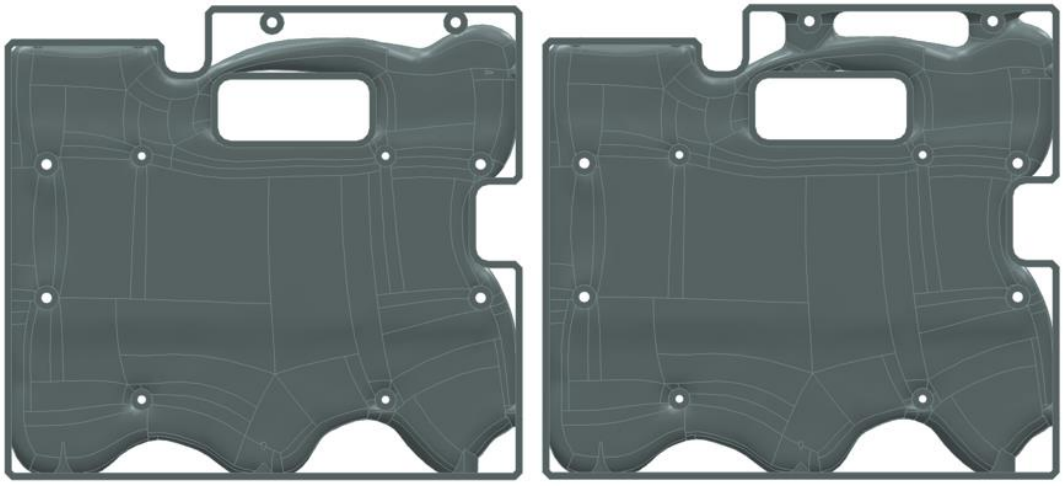

Figure 12. Initial unsupported bolthole design (left) and reinforced bolthole design (right).

The reinforced design weighs 433.11 g which is 1.7% lighter than the first topology optimized solid model. To achieve a lighter panel than the original rib type design, the researchers converted the optimized panel into lattice design. Since the mesh that was generated by nTopology varies from high density to low density on the boltholes, the researchers generated a surface lattice based on the mesh. Furthermore, since the design is not flat and includes sloping features, the surface lattice needs to be trimmed to enable proper contact of the components to the panel as illustrated in Figure 13.

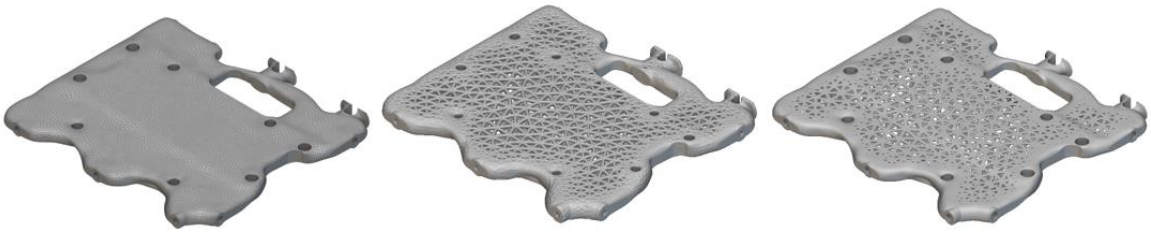

Figure 13. Mesh pattern of the optimized panel (left), Surface lattice (middle), and trimmed surface lattice (right).

As for the internal features of the panel, it was then converted to a uniform density BCC lattice since it requires the least number of struts among the three designs (Figure 14). Furthermore, it would allow the researchers to conduct structural verification on the lattice struts using selected regions or cells due to the limitation in computing capability of the available hardware.

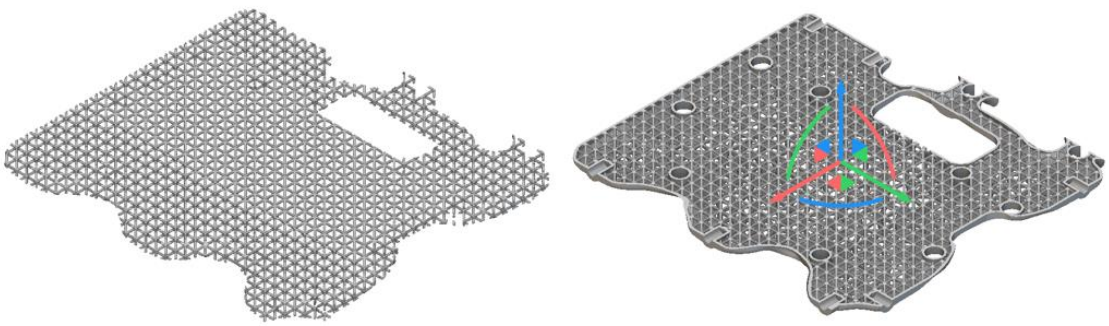

Figure 14. Internal lattice structure of the panel.

 doi:10.20944/preprints202604.1882.v1

To accommodate the mounting locations, the perimeter shell and bolt holes were merged (Figure 15) to the generated design. The result of the model, the final design (Figure 16) weighs 185.7 g which is lighter by 11.4 % from the original rib type design weighing 209.6 g and 65.2% from the solid panel weighing 533.3 g.

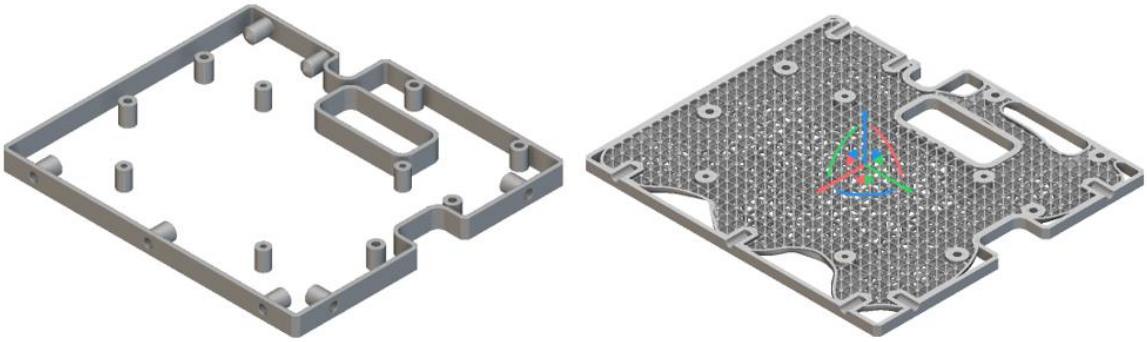

Figure 15. Internal lattice structure of the panel.

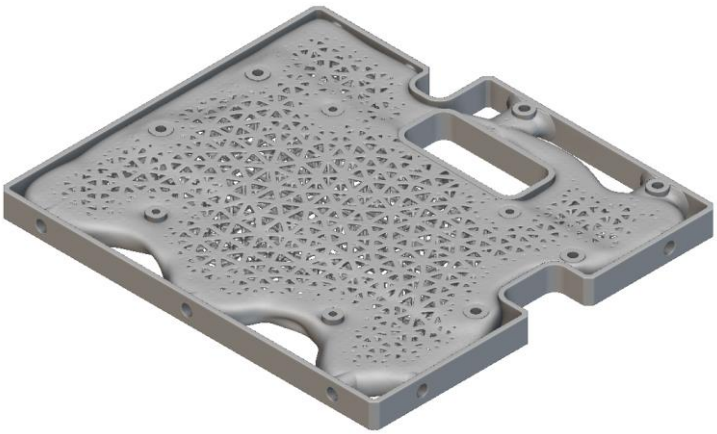

Figure 16. Final design of the lattice panel.

3.3. Finite Element Analysis (FEA) Verification

FEA was conducted to validate the structural integrity of the optimized designs. Initial static analysis of the merged topology-optimized solid model under revised load conditions (up to 24.44 N) indicated maximum stresses of 63.5 MPa concentrated near bolt holes. This value is well within the yield strength of the AlSi10Mg material (230–270 MPa as manufactured).

With the final design selected, the researchers verified the lattice design integrity using Finite Element Analysis in nTopology. Due to limitations in the software and hardware, the researchers were only able to verify a single cell or a 3 x 3 cell of the lattice design and not as a whole panel. This is because of the number of faces that will need to be generated due to the complexity of the lattice design.

The simulation verification uses a 3 x 3 lattice cell with a bolt hole at the center as illustrated in *Figure* 17. This is to simulate the behavior of the mounting once the loads are applied. The section measures 15 mm x 15 mm with an overall height of 10 mm. The section has a 1 mm thick top faceplate.

 doi:10.20944/preprints202604.1882.v1

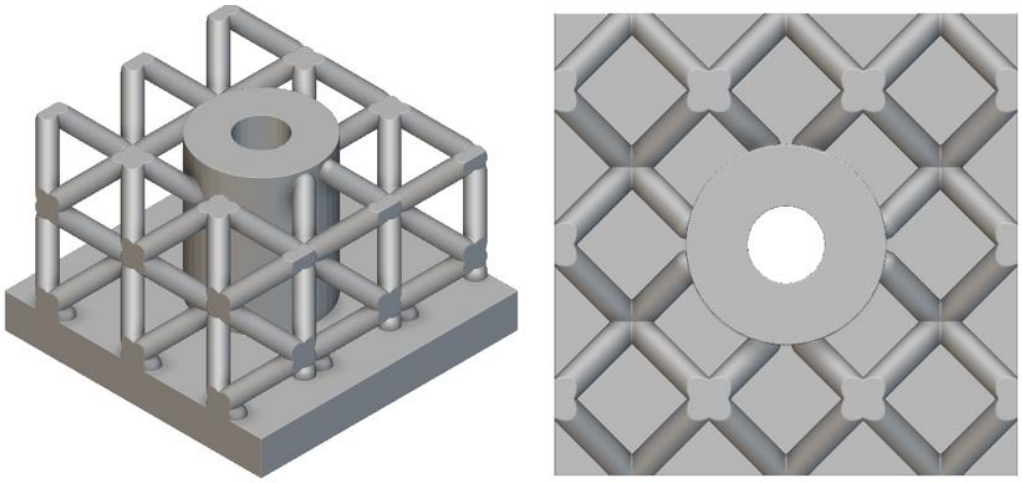

Figure 17. 3 x 3 Lattice Cell Verification Model.

All force component loads were added and concentrated inside the bolt hole in the center of the 3 x 3 lattice cell. Meanwhile, its displacement restraints were applied on the sides of the faceplate X Component, Y Component, Z Component are ± 31.78 N : ± 38.13 N: ± 31.78 N respectively.

The result of the simulation verification force application and displacement constraints (Figure 18) has shown that the section's maximum displacement was only 0.0009 mm while its maximum stress was only 15.47 MPa (Figure 19). This shows that for a 3 x 3 section of the lattice panel with the loads concentrated on it, it was able to withstand the loading conditions further justifying the use of BCC lattice rather than Octet. With the BCC lattice, it was able to withstand the loading conditions while reducing the maximum weight possible. To further verify the lattice design, the researchers conducted the same simulation for the remaining 8 possible combinations for the directions of the force components.

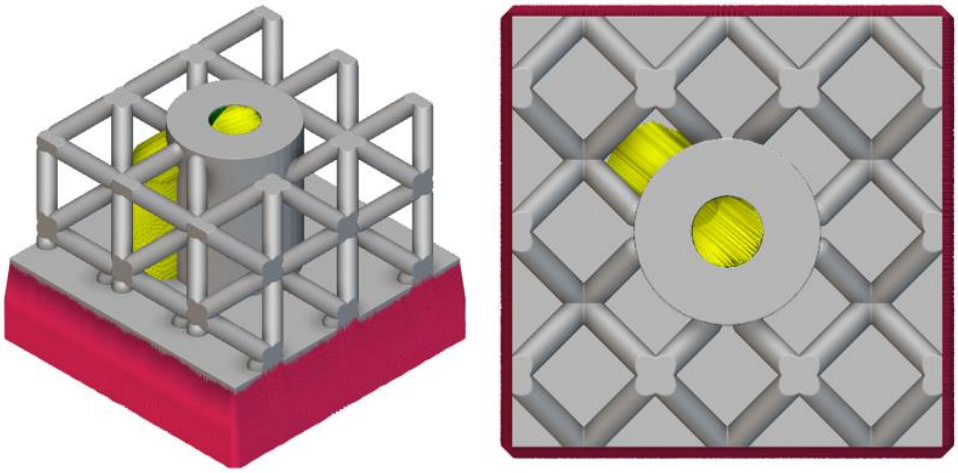

Figure 18. Force applications (yellow) and displacement constraints (red) for the verification.

 doi:10.20944/preprints202604.1882.v1

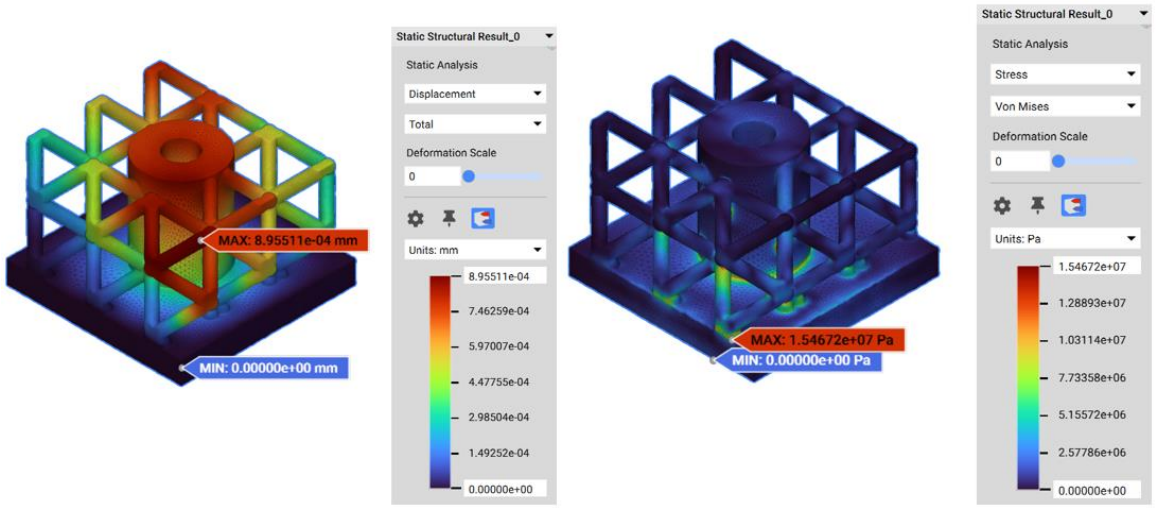

Figure 19. Simulation verification displacement (left) and stress (right) result.

All simulation iterations made prove that the BCC lattice design can withstand the loading conditions provided. In addition, the lattice design exhibits the greatest weight reduction among the three selections but structurally enough for the given loading conditions.

3.4. Printing Process and Fabrication

The process flow of printing in the EOS M290 starts by fixing the STL files. Materialise Magics is used in preparing the files (Figure 20). Part of the file preparation is the support generation on the files to be printed. Also, in this software, print orientation of the file is maximized, choosing the orientation where support structures and the print time is the minimum.

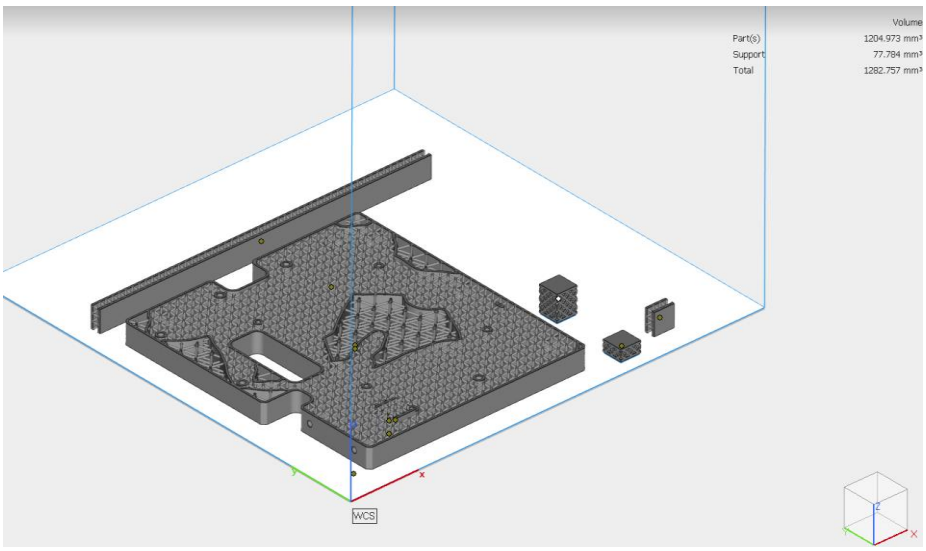

Figure 20. File preparation on the Materialise Magics Software.

The EOS M290 was set-up by preparing the build platform. This was conducted by levelling and setting the build platform on the platform carriage. The recoater was changed from a hard recoater to a soft recoater. A soft recoater was used in printing lattice structures so that the recoater will not damage the fine structures of the lattice during the printing process. After this, an initial layer of powder around 50 microns was spread onto the build platform, setting up the first layer of the printing. The print job was then transferred to the machine from the EOSprint workstation. The print job was then started through the machine's interface, where the machine establishes initial conditions such as build platform temperature, oxygen chamber concentrations and pressure differential in the

 doi:10.20944/preprints202604.1882.v1

build chamber and filter chamber. After establishing these conditions, the machine will start to eject laser onto selected areas on the build platform fusing the metal powders and then the machine will recoat another layer of powder and then eject again another layer. This process will be done repeatedly until the desired part is printed. Throughout the whole process, there is a constant supply of argon to the chamber in order for the aluminum to avoid chemical reactions and avoid thermal deformation leading to successful prints as shown in Figure 21.

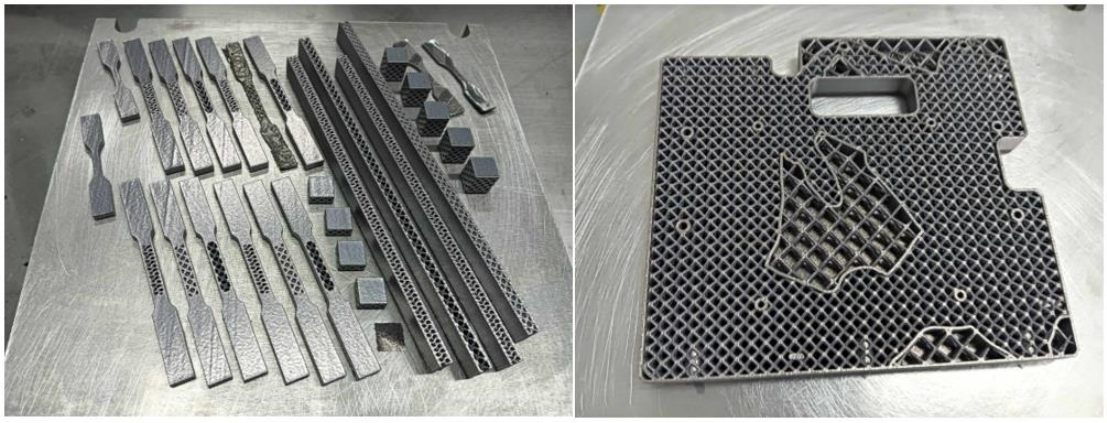

Figure 21. Flexural, Tensile, and compression printed outputs (left) and BCC panel printed output (right).

3.5. Mechanical Testing Results

Mechanical characterization involved compressive, tensile, and flexural testing of BCC, Octet, and Gyroid lattice specimens. Testing of single-layer lattice specimens revealed that the Gyroid lattice exhibited the highest average compressive load at 13,825.8 N. This was followed by the Octet lattice (10,736.4 N) and the BCC lattice (9,816.2 N). Notably, specimens printed with the optimized 30-micron layer height showed a significant increase in breaking load compared to the 40-micron batch, underscoring the importance of print parameter optimization. Tensile tests yielded an average maximum load of 5,183.9 N for the Octet lattice and 5,158.9 N for the Gyroid lattice. The BCC lattice recorded a lower tensile strength of 3,634.3 N.

4. Summary

The mechanical testing results highlight a trade-off between strength and weight. While the Gyroid and Octet lattices demonstrated superior compressive and tensile strength, the BCC lattice was ultimately selected for the final panel design. The BCC configuration offered the greatest potential for mass reduction, achieving the project's lightweighting goals more effectively than the heavier Octet or complex Gyroid structures (Figure 22). Despite having lower strength values than the Gyroid and Octet, the BCC lattice's performance (compressive load ~9,816 N) far exceeded the operational load requirements derived from the 9G and revised load cases. FEA verification confirmed that the BCC design maintains a high factor of safety.

 doi:10.20944/preprints202604.1882.v1

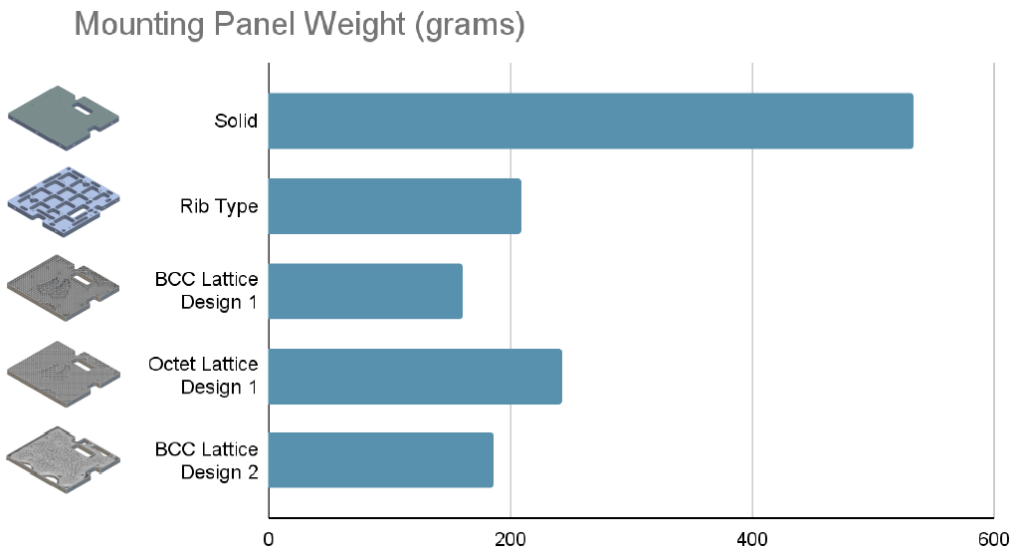

Figure 22. Summary of weights of mounting panel designs.

The study also demonstrated that DMLS is a viable manufacturing method for these complex geometries, provided that specific process controls, such as using a soft recoater and finer layer heights, are implemented to maintain strut integrity. The final fabricated panel achieved TRL-6, having been validated through both simulation and physical testing in a relevant environment.

5. Conclusions

This study successfully demonstrated the feasibility of developing lattice-based panels for satellite applications using Direct Metal Laser Sintering (DMLS). By leveraging Additive Manufacturing (AM) and topology optimization, the research established a viable alternative to traditional manufacturing methods for aerospace lightweighting.

A critical outcome of this work was the successful implementation of an alternative design approach shifting from a conventional fully enclosed sandwich structure to a one-sided solid panel design. This strategic modification was chosen for practicality, specifically to facilitate post-processing activities such as the removal of residual metal powder, which is a common challenge in closed-cell AM structures. This design approach resulted in a final lattice panel weight of 185.7 g, achieving a 11.4% weight reduction compared to the original rib-type design (209.6 g) and a substantial 65.2% reduction compared to a solid panel (533.3 g).

The structural reliability of the fabricated panel was validated through a convergence of Finite Element Analysis (FEA) and physical mechanical testing. FEA simulations under revised flight load conditions confirmed that the maximum stress induced in the BCC lattice structure (approximately 15.47 MPa) remained significantly below the yield strength of the AlSi10Mg material (230 MPa as manufactured).

Experimental Validation: This simulation data was corroborated by physical testing of "dog bone" tensile specimens. The BCC lattice specimens demonstrated a tensile load capacity of 3,634.3 N. Although the Gyroid and Octet lattices exhibited higher tensile limits (averaging over 5,000 N), the BCC lattice was determined to possess sufficient strength to withstand the calculated flight loads while offering superior manufacturability and weight savings.

Process Parameters and Lattice Selection The study highlighted the critical importance of optimizing printing parameters. The use of a soft recoater blade and a finer 30-micron layer height (opposed to 40 microns) proved essential in preserving the integrity of intricate lattice struts and improving surface finish. While Gyroid structures offered superior strength, the BCC lattice was ultimately selected as the optimal architecture for this specific application due to its balance of weight reduction, compliance with JAXA stiffness requirements, and ease of powder removal.

 doi:10.20944/preprints202604.1882.v1

Local Manufacturing Feasibility and Future Work The successful fabrication and verification of these panels, achieving Technology Readiness Level 6 (TRL-6), underscore the feasibility of utilizing locally manufactured lattice-based structures for CubeSats. However, future work must further address post-processing challenges. Specifically, optical inspections revealed residual powder adhering to lattice struts, indicating that more rigorous cleaning techniques are required. Furthermore, while the current prototype met design specifications, continuous monitoring of dimensional accuracy and tolerance through precision metrology remains vital to ensure seamless integration with satellite buses like the PHL-50.

Funding: This research was funded by the Department of Science and Technology – Philippine Council for Industry, Energy and Emerging Technology Research and Development (DOST–PCIEERD), with facility support from the Department of Science and Technology – Metals Industry Research and Development Center – Advanced Manufacturing Center (DOST–MIRDC AMCen). The APC was not externally funded.

Data Availability Statement: The data presented in this study are available on reasonable request from the corresponding author.

Acknowledgments: The authors gratefully acknowledge the Department of Science and Technology – Philippine Council for Industry, Energy and Emerging Technology Research and Development (DOST–PCIEERD) for funding support, the Department of Science and Technology – Metals Industry Research and Development Center – Advanced Manufacturing Center (DOST–MIRDC AMCen) for providing research facilities, and Engr. Fred P. Liza for the endless support and guidance. The authors also acknowledge Engr. Abrey Angelo L. Arroyo and Engr. Jose Emmanuel D. Ignacio for assisting in the formatting of the article for submission.

Conflicts of Interest: The authors declare no conflicts of interest. The funders had no role in the design of the study; in the collection, analyses, or interpretation of data; in the writing of the manuscript; or in the decision to publish the results.

References

1. Siengchin, S., A review on lightweight materials for defence applications: Present and future developments. Defence Technology, 2023. **24**: p. 1-17.
2. Dine, F. and S. Gasmi, Biodegradable Polymers in 3D Printed Aerospace Components: Design Optimization for Structural Integrity. 2024.
3. Alhembar, A., et al., Optimizing the specific mechanical properties of lattice structures fabricated by material extrusion additive manufacturing. Journal of Materials Research and Technology, 2023. **22**: p. 1821-1838.
4. Sheikhi, M.R., et al., Force attenuation performance in sandwich structures with STF and M-STF encapsulation. Heliyon, 2024. **10**(5): p. e27186.
5. Wang, Z., *Recent advances in novel metallic honeycomb structure.* Composites Part B: Engineering, 2019. **166**: p. 731-741.
6. Boschetto, A., et al., *Additive Manufacturing for Lightweighting Satellite Platform.* Applied Sciences, 2023. **13**(5): p. 2809.
7. Georges, H., et al., Mechanical Performance Comparison of Sandwich Panels with Graded Lattice and Honeycomb Cores. Biomimetics, 2024. **9**(2): p. 96.
8. Mat Samudin, I., et al., Stress strain curve analysis of sheet based TPMS structures in quasi static compression test: A review. Journal of Materials Research and Technology, 2025. **36**: p. 5757-5796.
9. Pan, C., Y. Han, and J. Lu, *Design and Optimization of Lattice Structures: A Review.* Applied Sciences, 2020. **10**(18): p. 6374.
10. Yu, Z., et al., Current research status on advanced lattice structures for impact and energy absorption applications: A systematic review. Thin-Walled Structures, 2025. **215**: p. 113490.
11. Obadimu, S. and K. Kourousis, Compressive Behaviour of Additively Manufactured Lattice Structures: A Review. Aerospace, 2021. **8**: p. 207.

 doi:10.20944/preprints202604.1882.v1

12. Khan, N. and A. Riccio, A systematic review of design for additive manufacturing of aerospace lattice structures: Current trends and future directions. Progress in Aerospace Sciences, 2024. **149**: p. 101021.
13. Bouzoukis, K.-P., et al., *An Overview of CubeSat Missions and Applications.* Aerospace, 2025. **12**(6): p. 550.
14. Raja, A., et al., A review on the fatigue behaviour of AlSi10Mg alloy fabricated using laser powder bed fusion technique. Journal of Materials Research and Technology, 2022. **17**: p. 1013-1029.
15. Kunisetti, P. and B. Prasad, A detailed study on optimizing DMLS process parameters to enhance AlSi10Mg metal component properties. Journal of Engineering and Applied Science, 2024. **71**.